Journal of Urban and Environmental Engineering, v.8, n.2, p.211-217

ISSN 1982-3932
doi: 10.4090/juee.2014.v8n2.211217

Journal of Urban and Environmental Engineering

www.journal-uee.org

FINITE ELEMENT MODELING OF THE CRACK PROPAGATION IN RC BEAMS BY USING ENERGY APPROACH

Shahriar Shahbazpanahi* and Chia Paknahad

Department of Civil Engineering, Islamic Azad University, Sanandaj Branch, Iran

Received 18 March 2014; received in revised form 10 December 2014; accepted 11 December 2014

Abstract: In present study, an interface element with nonlinear spring is used to simulate cohesive zone model (CZM) in reinforced concrete (RC) beam for Mode I fracture. The virtual crack closure technique (VCCT) is implemented to model the propagation of the fracture process zone (FPZ). This model can be calculated the energy release rate by using new method from energy approach. Energy dissipation rate by steel bars is obtained to effect on the crack propagation criterion to implement in finite element method. The numerical results are compared with references result available in the literature. It is observed that the FPZ is increased linearly and then stay constant. It may be due to effect of steel bars or inherent behavior of FPZ. The results show that the proposed model does not depend on mesh size.

Keywords: FPZ; stiffness; RC beams; energy release rate

* Correspondence to: Shahriar Shahbazpanahi, Tel.: +98 918 871 0936; Fax: +98 871 328 8684.
E-mail: sh.shahbazpanahi@gmail.com

INTRODUCTION

Crack modeling in reinforced concrete (RC) beam is essential due to nonlinear behavior. One of the challenges is the propagation of tensile crack in RC beam. There is a little knowledge on how to predict crack in RC beam. However many significant efforts have been made to study fracture mechanics in failure mode of RC beams (Prasada & Krishnamoorthy, 2002; Yang & Chen, 2005).

Fracture mechanics were employed to model tensile crack in concrete with strain softening behavior. Hillerborg *et al.* (1976) proposed the first model in concrete based on nonlinear fracture mechanics. The mentioned study introduces a region, often termed as fracture process zone (FPZ), ahead of real crack tip which leads to crack closure (**Fig. 1**). This significant and large zone contains micro-cracks in matrix–aggregate, gel pores, shrinkage cracks, bridging, and branch of cracks. The FPZ is located ahead of the macro-cracks. Since a significant amount of energy is stored in this region, a crack can have stable growth before peak load. In addition, the existence of the FPZ justifies the strain softening behavior in the stress- crack opening curve after peak load. In this region, the interlocking crack surfaces after the peak load contribute to a gradual decline in stress and prevent sudden failure (Esfahani, 2007). The FPZ dimension depends on the size of the structure, initial crack, loading and material properties of concrete. The length of the FPZ is of special interest as compared to its width.

Energy approach can describe the crack propagation state in the fracture process at the crack-tip. The energy approach displays that the energy required, to form crack, it is called energy release rate, must be enough to overcome the critical fracture energy. A criterion for crack propagation can be defined in terms of energy release rate to study crack state. The energy approach criterion depends on stiffness matrix, displacement and crack geometry (Xie & Gerstle, 1995).

Different approaches have been investigated to model discrete crack as well as its propagation criteria. To simulate the FPZ, Hillerborg *et al.* (1976) used cohesive stress which is a function of crack opening. Hillerborg's approach can be applied to any structure, even if no notch or fictitious crack exists (Anderson, 1991). In this model, as stress is a function of crack opening, it reaches tensile strength at the tip of the crack, and reduces to zero at its critical opening (w_c). The amount of the area under the stress-crack opening curve is equal to energy release rate. This model, often referred to as cohesive zone model (CZM), was deployed to simulate the FPZ in normal size structures, using either nodal force release method or interface element with zero initial thickness technique (Yang & Liu, 2008).

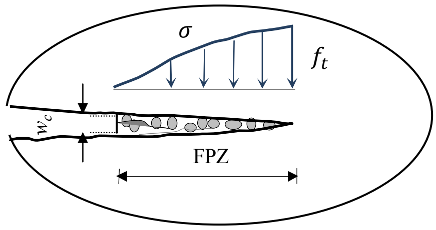

Fig. 1 The FPZ in front of crack with normal stress.

So far, the method suggested by Hillerborg *et al.* (1976) has been applied more widely due its practically, accuracy and cost effectiveness. To model the CZM, two types of interface elements were deployed. One of the most widely used interface elements is continuum cohesive zone model (CCZM). An alternative interface element is discrete cohesive zone model (DCZM) which is very simple to implement. The DCZM results are satisfactory compared to CCZM, especially for pre-cracking phase when stiffness is selected to have a very large value (Xie & Waas, 2006). The DCZM is based on the basic idea that cohesive zone behaves like a spring. This point of view suggests that instead of using a 2-D interface element along the crack path, a spring element should be utilized between interfacial node pairs. In the present investigation DCZM is applied because this method reduces computational time and is compatible with the finite element method.

From finite element point of view, stiffness of FPZ should be properly chosen. In practice, this damage zone has a different stiffness due to micro-cracking, bridging, branching that undertake use of energy in crack growth. So it is significant to use more accurate stiffness element to simulate the FPZ in finite element method.

Also, to predict crack propagation, correct estimation of energy release rate is important. As it is known, energy release rate is the basic idea of nonlinear fracture mechanics for crack propagation that depends on many parameters such as external load and element stiffness.

On the other hand, steel bars have usually been applied to improve flexural capacity and to rest crack growth in the concrete. So, modeling the steel bars and its effect on propagation of tension cracks in RC beam is necessary.

In the present study, an interface element is utilized to simulate cohesive cracks. This model justifies the softening behavior of normal stress in the FPZ in concrete. The virtual crack closure technique (VCCT) is applied to model the propagation of the fracture process zone. A nonlinear spring element is used to derive forces in nodes due to normal stress in the FPZ. Strain energy release rate is obtained by energy approach while effect of steel bars on propagation of tension crack criterion is considered. Results for RC beam with initial notch are presented and comparisons between computed and experimental recent results are made.

NUMERICAL MODEL

Interface element

As mentioned before, the FPZ has a softening behaviour due to the interlock of aggregates and micro-cracks. Thus, a nonlinear spring is proposed to place between interfacial node pairs (**Fig. 2**). In this figure, the node pairs '1' and '2' have initially the same coordinates. Spring softening is set at the crack tip between the nodes '1' and '2'.

The local element stiffness matrix and the displacement vector related to nodes '1' and '2' are given by:

$$\mathbf{K} = \begin{bmatrix} k_x & 0 & -k_x & 0 \\ 0 & k_y & 0 & -k_y \\ -k_x & 0 & k_x & 0 \\ 0 & -k_y & 0 & k_y \end{bmatrix}, \mathbf{u} = \begin{Bmatrix} u_1 \\ u_2 \\ u_3 \\ u_4 \end{Bmatrix} \quad (1)$$

where k_x and k_y are the stiffness values related to the local coordinates in x and y directions, respectively. Also, u_1 and u_2 are displacement components in x and y directions for node '1', u_3 and u_4 are displacement components in x and y directions for node '2', respectively. In this research, the value of the stiffness in x direction, k_x , is obtained based on the normal stress versus crack opening curve. **Figure 3** illustrates the normal stress versus crack opening curve. The normal stress can be explained as (Kumar & Barai, 2011):

$$\sigma = f_t\, exp(-\, k\, w^{\lambda}) \quad (2)$$

where σ, f_t and w are normal stress, tensile strength of concrete and crack opening, respectively .The k , λ are constant. Thus stiffness in x direction, k_x, can be calculated as:

$$k_x = \frac{1}{k\, \lambda\, f_t\, exp(-\, k\, w^{\lambda})}. \quad (3)$$

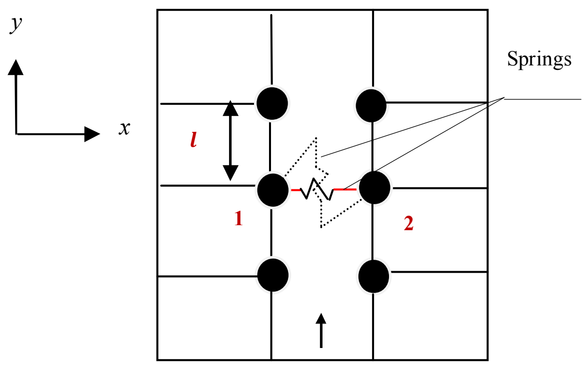

Fig. 2 The spring interface element between two nodes.

Small displacements are assumed to model crack. Based on small displacements, the stiffness at ith iteration ($i = j + 1$) in nonlinear solution can be written as:

$$k_x^{\,i} = \frac{1}{k\, \lambda\, f_t\, exp\, (-\, kw_j^{\,\lambda})} \quad (4)$$

where the w_j is crack opening in jth iteration. For fast convergence on nonlinear solution, the initial stiffness is used as $w_c/30$ by small time step in nonlinear solution. where w_c is critical opening displacement.

Since only Mode I is considered and the crack path is known, the stiffness component in y direction can be calculated from shear modulus of the concrete (Xie & Waas, 2006).

Energy release rate

The strain energy for mth element, U_m, is the hatching area under σ –COD curve (**Fig. 3**):

$$U_m = \int_0^{w^j} f_t\, exp\left(-\, k\, w^{\lambda}\right) d\, w \quad (5)$$

that can be calculated by using Gaussian integration in finite element method. The strain energy release rate for Mode I fracture, G_I, based on energy approach is:

$$G_I = \frac{U_m - U_{m-1}}{B\Delta} \quad (6)$$

where A and B are crack surface area and thickness of the beam. U_{m-1} is the strain energy for $(m\text{-}1)th$ element. The Δ is crack extension which in the present study is assumed (Esfahani, 2007):

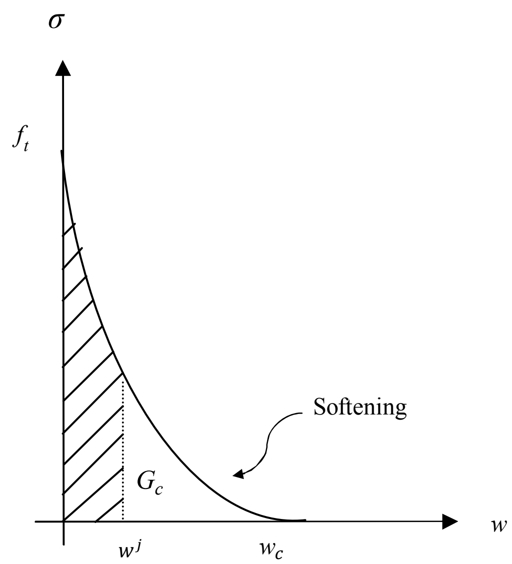

Fig. 3 Concrete σ –COD curve

$$\Delta = 0.4 \frac{n' E G_c}{f_t^2} \quad (7)$$

where the n', E and G_c are number of elements with changes their stiffness behind the FPZ, elasticity modulus of the concrete and critical strain energy release rate, respectively. At each step, more than one element may deal with crack extension and it propagates along the other elements.

As for the steel bar to resist crack propagation, in the present study, energy dissipation rate based on energy approach, as surface force in (Xie & Gerstle, 1995), is obtained by:

$$R = \frac{\partial (u_9{}^m - u_{11}{}^m) F_x}{\partial A} \quad (8)$$

where the F_x is nodal force due to existing steel bar in x direction. The $u_9{}^m$ and $u_{11}{}^m$ are displacements in x direction for node '5' and '6', respectively, in the vicinity of steel bar (**Fig. 4**), for mth element due to propagation of the FPZ in the concrete.

The F_x due to propagation of the FPZ in the steel bar, for mth element is given by:

$$F_x = k_s \left(u_9{}^m - u_{11}{}^m \right) \quad (9)$$

where the k_s is elastic modulus of steel bar.

Substituting **Eq. (9)** into **Eq. (8)** and using finite deference method yields:

$$R = \frac{k_s [(u_9{}^m - u_{11}{}^m)^2 - (u_9{}^{m-1} - u_{11}{}^{m-1})^2]}{(\frac{A_s}{B})\Delta} \quad (10)$$

where the A_s is cross-section area of steel bar. Eq. (10) is used to estimate effect of steel bars as crack propagates in the concrete. This relationship shows that initially when the FPZ length increases and crack opening mouth is small in concrete, effect of steel on preventing crack propagation is less. Finally, as the FPZ length reaches the constant value and crack opening mouth increases; steel bar role is to resist crack growth increases. So far, no model has presented a convincing equation to estimate effect of steel bar on crack propagation. The energy criterion of crack propagation will be:

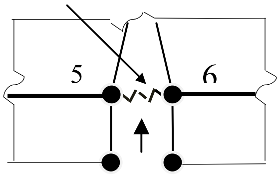

Fig. 4 Interface element to model steel bars.

$$G_I - R > G_{Ic} \quad (11)$$

where G_{Ic} *is* critical strain energy release rate. It is noted that the R and G_{Ic} are not based on the size of the mesh.

Stress-free region

A more accurate explanation of propagation and crack formation must be considered in model such as stress-free region length. Wu *et al.* (2011) shown as crack opening displacement reaches to 3.6 G_c/f_t, stress-free region appears in front of the notch tip while FPZ length increases linearly and fully develops. That means as crack length reaches about 0.91 times the ligament length, $h - a_0$, FPZ length increases linearly and fully develops.That is formulated in finite element methods by:

$$a_{\sigma=0} = n\, l \quad (12)$$

where n and l are number of elements that have failed behind crack and length of mesh. When FPZ fully propagated, n element is set to zero behind FPZ as crack propagates.

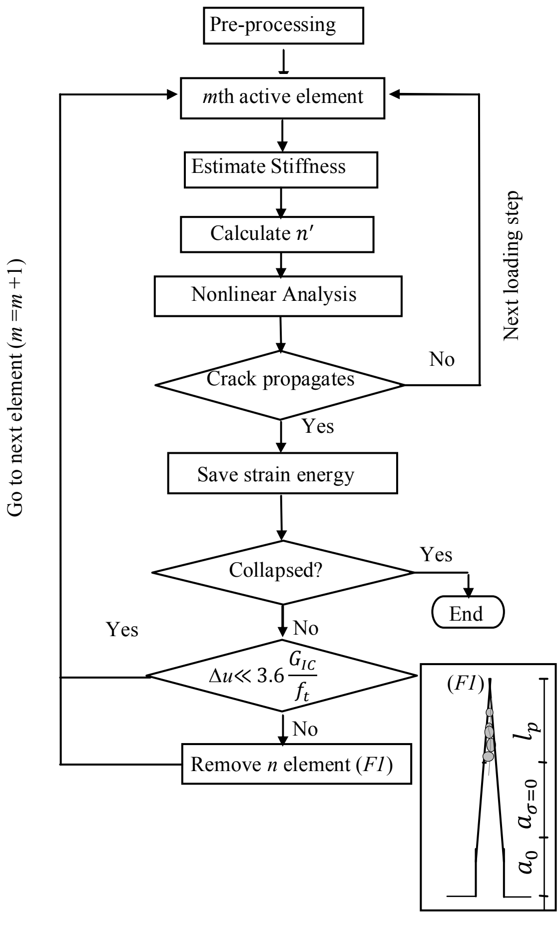

Fig. 5 Flowchart of fracture in m th element.

Computer implementation

FEAPpv program code is developed for analysis of 2-D plane stress in concrete (Taylor, 2009). Nonlinear spring is implemented for interface element in the User Subroutine FEAPpv Fortran programming while nonlinear dynamic relaxation method is used for interface element in the program. Four-node isoparametric elements are used for bulk concrete as linear elastic. Two-node truss element is used to model steel bar with perfect plastic behaviour. Bond-slip between longitudinal bars and concrete is modelled by Ingraffea *et al.* approach (1984). **Figure 5** showed the major step in the present numerical model to solve fracture in the beam.

RESULTS AND DISCUSSION

The example is a reinforced concrete beam with simple supports (**Fig. 6(a)**) which experimental data were replicated by Prasad and Krishnamoorthy (2002). The geometry of the RC beam is 1220 mm length, 125 mm thickness. Material properties are 29270 MPa elastic modules, 0.18 Poisson ratios and 30.1 MPa compressive strength of concrete, 0.3 Poisson ratio, 100.48 mm^2 cross-section area and 395 MPa yield strength of steel. Tensile strength for concrete is 4.11 MPa, G_c=113 N/m and crack opening displacement critical is 0.15 mm. The k and λ are 1.01 and 0.063. The initial mesh is illustrated in **Fig. 6(b)**. Load versus deflection at the mid-span of the beam in present study is compared with experimental result and previous model in **Fig. 7** (Prasada & Krishnamoorthy, 2002). **Figure 7** shows that the results are close to experimental data. It is seen that the stiffness of the beam in present study is slightly less than the previous model observation (Prasada & Krishnamoorthy, 2002). This difference may be acceptable as plastic deformation of steel and its effect of crack propagation is considered in present model. It may be seen that the effect of steel bars on crack propagation has an important role on the crack behavior of the beam.

Figure 8 shows crack patterns at load 26 KN in present study. Stress-free region length is 6.1 mm while FPZ length is 130.9 mm. The crack mouth opening is 0.481 mm while deflection at the mid-span is 0.534 mm at mentioned load. The FPZ propagation reaches almost three-fourth of the beam depth by fifth step of loading. At seventh step of loading the FPZ is fully propagates and stress-free region length appears. Initially the crack mouth opening increases gradually and then stays stable due to effect of steel bars as load increases. At the final stage, crack mouth opening increases rapidly due to the bond-slip of the steel bars.

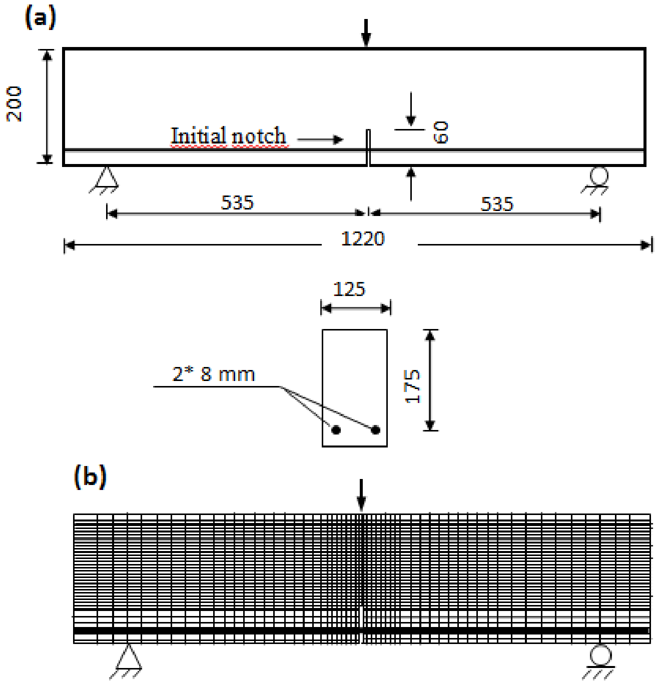

Fig. 6 (a) The notched RC beam (Unit: mm) **(b)** Initial mesh with 42 interface element.

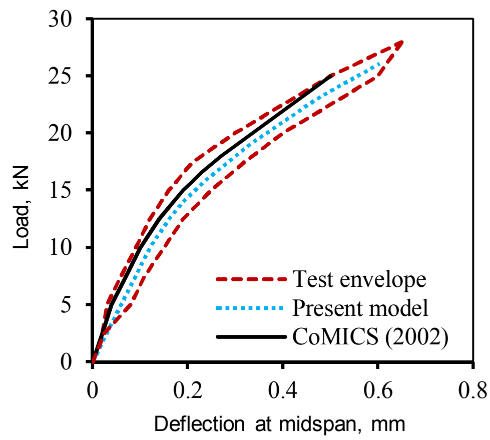

Fig.7 Load-deflection at the mid-span.

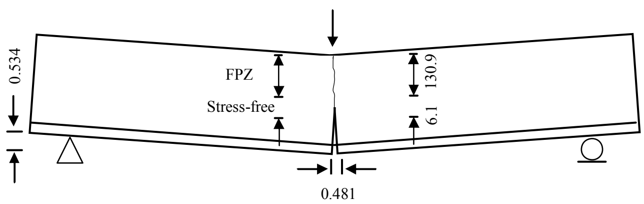

Fig.8 Final crack predicate scale=150 (Unit: mm).

Figure 9 indicates load versus deflection at mid-span curve with three size meshes compared with experimental envelope (Prasada & Krishnamoorthy, 2002). Mesh (1) has 102 interface elements; mesh (2) has 76 interface elements, and (c) has 42 interface elements. The approximate matching of the three curves demonstrates the independence of the model from mesh size and shows the model has fast convergence.

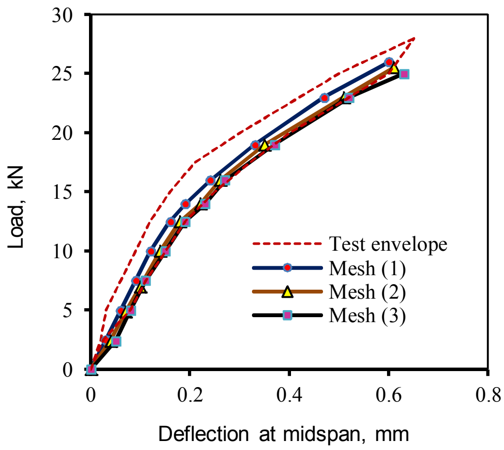

Fig. 9 Load-deflection with three size meshes.

Fig. 10 shows how the FPZ length is changed as the load increases by different cross-section area of steel bars.It can be seen that the FPZ is increased linearly and then stay constant. It may be due to effect of steel bars or inherent behavior of FPZ (Xu *et al.*, 2011). As expected, when cross-section area increases, the load bearing capacity increases at the same FPZ length. It is also observed that effect of the increasing steel bars cross-section area is more at higher loads.

The second example is a reinforced concrete beam with simple supports which is first tested by Bresler and Scordelis (1963) and analyzed by Arrea and Ingraffea (1984) in **Fig. 11**. The geometry of the RC beam is 4572 mm length, 305.8 mm thickness. Material properties are 24000 MPa elastic modules, 0.18 Poisson ratios for concrete and 200 GPa elastic module, 0.3 Poisson ratio, 3290 cross-section area, 552 MPa yield strength of steel. Tensile strength of concrete is 2.8 MPa and crack opening displacement critical is 0.152 mm. A two-node truss element with elastic-perfectly plastic behaviour is used to model the steel bars. To model the symmetry condition, half of the beam is simulated only. Bond-slip between bars and concrete is assumed to be perfect. Also, the crack in RC beam is managed by a primary crack, (first introduced by Ingraffea *et al.* (1984) where the reinforcing bar crosses a primary crack.

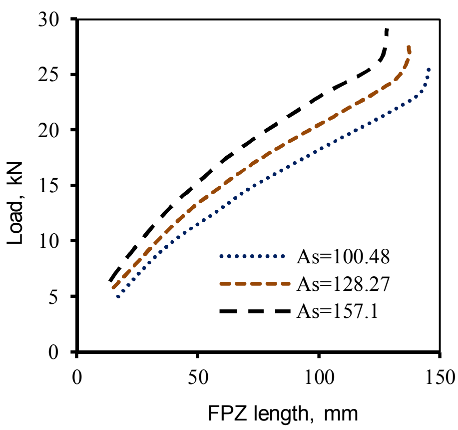

Fig. 10 Load versus the FPZ length with different cross-section area of steel bars.

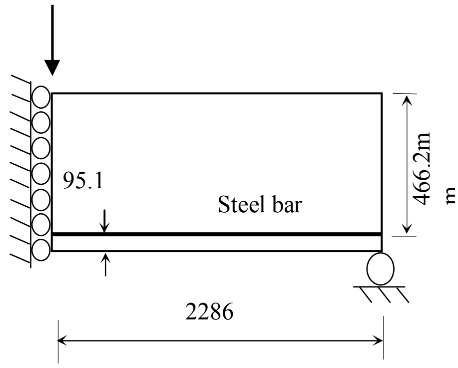

Fig. 11 Half of the RC Beam (Unit: mm).

Load versus deflection at the mid-span of the beam in the present study is compared with experimental data (Bresler & Scordelis, 1963) and analyze results by Arrea and Ingraffea (1982) in **Fig. 12**. It can be seen clearly that the shapes of the curves are similar to the experimental data. It is seen that the stiffness of the beam in the present study is more than experimental observation. This is unavoidable because the plasticity of concrete, compression cracking, the bond-slip of bar-concrete and mixed mode of crack propagation has not been considered in the present model. In the present study the effect of steel bars does not occur up to 100 kN. Beyond this point, the cracks take place and steel bars have influence. At a load of 285 kN, the stress in the reinforcement bars reaches the yield stress.

Crack patterns are shown in **Fig. 13(a)** in the experimental study by Bresler & Scordelis (1963) and crack paths are illustrated by the present study in **Fig. 13(b)** at load 285 kN. These figures illustrate that locations of flexural cracks obtained from the present model and experimental data are very close.

It can be seen that in the present model the shear crack near the support is not predicted. This is perhaps due to Mode I of crack propagation that can only modeled in the present study and just the flexural cracks is allowed to start. Further research is needed to model shear crack by considering mixed mode.

In the present model, initially a few flexural cracks occur near the mid-span at a load 100 kN. These initial cracks start to propagate and crack widths increase, as the load increases. A few cracks as far from the mid-span are also started behind this load. When the load is about 185 kN, the first crack propagates with a length of about 297 mm. Experimental predicted 13 cracks including flexural and shear cracks while in present model 10 flexural cracks were predicted.

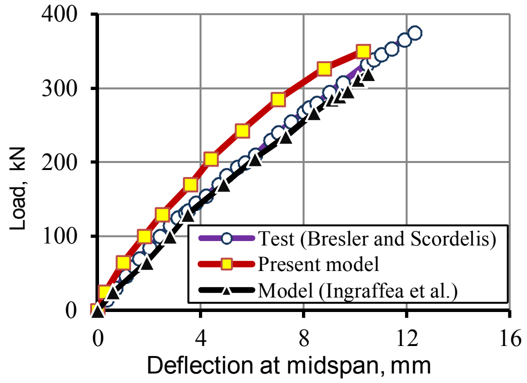

Fig. 12 Load-deflection at the mid-span.

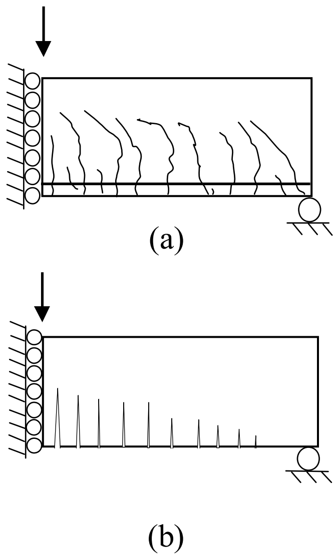

Fig.13. Crack predicted at 285 kN load
(a) Experimental (Bresler & Scordelis, 1963); **(b)** Present model

CONCLUSION

The present investigation proposes a simple approach to simulate cohesive crack in RC beam. In the present study, an interface element with nonlinear spring is used to simulate the CZM in beam to an accurate explanation of Mode I of crack propagation in RC beam. virtual crack closure technique (VCCT) is implemented to simulate the development of the FPZ and stress-free region length of the fracture. An accurate element stiffness matrix is applied to derive the forces in nodes due to normal stress in the FPZ. By using this model, energy release rate is calculated directly by a new method. It is observed that the FPZ is increased linearly and then stay constant. It may be due to effect of steel bars or inherent behavior of FPZ. The model is easy, accurate, efficient and capable to model crack growth in RC beam. The model decreases the computational time and complexity of discrete crack.

REFERENCES

Anderson, T. (1991) *Fracture mechanics fundamental and application.* CRC Press Inc., Boca Raton(FL), USA.

Arrea, M. & Ingraffea, A. R. (1982) *Mixed-mode crack propagation in mortar and concrete.* Cornell University: Report No. 81-13, Department of Structural Engineering.

Bresler, B. & Scordelis, A. (1963) Shear strength of reinforced concrete beams. *Amer. Concrete Inst.* **60**(40), 51-72.

Esfahani, M. (2007) *Fracture mechanics of concrete.,* Tehran Polytechnic press, Tehran, Iran.

Hillerborg, A., Modeer, M. & Petersson, P.E. (1976) Analysis of crack formation and crack growth in concrete by means of mechanics and finite element. *Cement Concrete Res.* **6**, 773-782.

Ingraffea, A., Gerstle, W., Gergely, P. & Saouma, V.(1984) Fracture mechanics of bond in reinforced concrete. *J. Structural Enging.* **110**(4), 1871-890.

Kumar, S. & Barai, S. V.(2011) *Concrete fracture models and applications*. Springer, Berlin Heidelberg, USA.

Prasada, M. & Krishnamoorthy, C.(2002) Computational model for discrete crack growth in plain and reinforced concrete. *Computer Methods in Applied Mechanics and Engineering,* **191**(2), 2699–2725.

Taylor, L.(2009) *FEAPpv source, A finite element analysis program, Personal version,* Berkeley, USA.

Wu, Z., Rong, H., Zheng, J. & Xu, F. (2011) An experimental investigation on the FPZ properties in concrete using digital image correlation technique. *Enging. Fract. Mechan.* **78**(17), 2978–2990.

Xie, D. & Waas, A.(2006) Discrete cohesive zone model for mixed-mode fracture using finite element analysis. *Enging. Fract. Mechan.* **73**(13), 1783–1796.

Xie, M. & Gerstle, W.(1995) Energy-based cohesive crack propagation modeling. *J. Enging. Mechan.* **121**(12), 1349-1458.

Xu, F., Wu, Z., Zheng, J., Zhao, Y., and Liu, K. (2011) Crack extension resistance curve of concrete considering variation of FPZ length. *J. Materials Civil Enging,* **23**(5), 703-710.

Yang, Z. & Chen, j.(2005) Finite element modelling of multiple cohesive discrete crack propagation in reinforced concrete beams. *Enging. Fract. Mechan.* **72**(14), 2280–2297.

Yang, Z. and Liu, G.(2008). Towards fully automatic modelling of the fracture process in quasi-brittle and ductile materials: a unified crack growth criterion. *J. Zhejiang University Sci. A,* **9**(7), 867-877.